

Uncoupled Multi-core Fiber Design for Practical Bidirectional Optical Communications

Tetsuya Hayashi, Takuji Nagashima, Ayumi Inoue, Hiroataka Sakuma, Takahiro Sugauma, Takemi Hasegawa
Optical Communications Laboratory, Sumitomo Electric Industries, Ltd., 1, Taya-cho, Sakae-ku 244-8588 Yokohama, Japan
Author e-mail address: t-hayashi@sei.co.jp

Abstract: We review and discuss the design factors and considerations on MCFs for bidirectional transmissions, including connection polarity and crosstalk requirements. We also introduce MCFs suitable for bidirectional long-haul and short-reach transmissions. © 2022 The Author

1. Introduction

Space division multiplexing (SDM) using multi-core fibers (MCFs) is a promising candidate for the next-generation optical fiber transmission technology both in long-haul submarine transmissions and in short-reach optical interconnects in data centers. To achieve higher core density and/or better optical performance in a limited MCF cross section, XT suppression by assigning opposite signal propagation directions between adjacent cores [1–7] is a very promising way to realize performance-improved practical MCF transmission systems, because most of today's full duplex optical fiber communication systems consist of optical fiber pairs to realize bidirectional transmissions.

In this paper, we briefly review common MCF design factors for unidirectional transmissions and bidirectional transmissions, and discuss design considerations on practical use and better performance in bidirectional transmissions. We also introduce fabricated MCFs in view of bidirectional transmission performance.

2. MCF design factors

Fig. 1 summarizes the design factors of MCFs. Index structure of each core affects the optical properties of each core (MFD, cutoff wavelength, chromatic dispersion, etc.), and is basically designed as well as SMF core design. Unique features of MCF design are core count, layout, and pitch, to be designed such that the coupling between the cores can be kept to a preferable level and the core density (core count per fiber cross section) can be increased. The so-called outer cladding thickness (OCT, the minimum distance between a core center and cladding-coating interface) is also important to suppress the leakage of the light to the coating in the operation wavelength band.

3. Design consideration on practical use and better performance in bidirectional transmissions

The above-mentioned design factors are well known and considered in most of MCF design proposals. In this section, we discuss other design factors for uncoupled MCFs, which are important to realize practical transmissions but often overlooked, or unique for bidirectional transmissions.

3.1. Connection polarity

Except for relatively simple long-haul networks like point-to-point submarine systems, the polarity management of MCF connections would be a challenge for installation and management of multipoint-to-multipoint MCF networks. Such a problem can be avoided by the line symmetric core layouts w.r.t. the line through the cladding center (center line), as shown in Fig. 2. The “key” direction is the center line direction toward the marker (core). Unique core ID layout is inverted w.r.t. the center line between the two ends of the MCFs; therefore, End A–End B connection is necessary to keep the unique core ID through a link. However, by accepting the core ID transpose at opposite ends (like Type B polarity of MPO), the same ends can be connected without considering polarity. For example, if we name the cores like “ L_n ” for the left cores and “ R_n ” for the right cores from the center line, L_n cores at one end are always R_n cores at the other end, and L_n cores are always mated to R_n cores both in the same end connection and different end connection. At MCF termination, if there are no cores on the center line (Fig. 2(a)), the identical core routings from fan-in/fan-out (FIFO) to transceivers (TRx) or the identical Tx and Rx layouts in native MCF TRx can be used for the both ends the MCF. If there are any cores on the center line (Fig. 2(b)), each end of the MCF must have different types of fan-in/fan-out (FIFO) devices or different layouts of TRx, which would make network

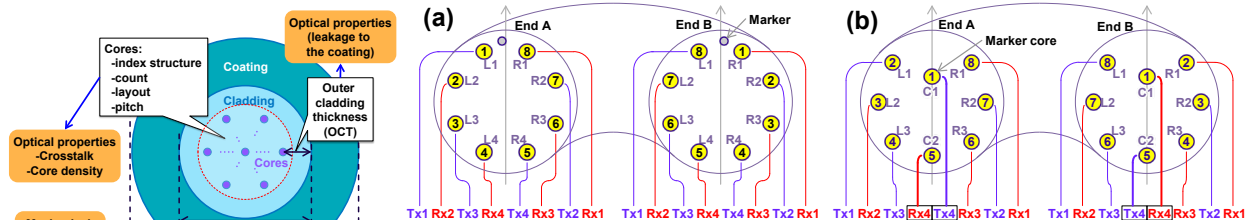


Fig. 1. Design factors of MCFs.

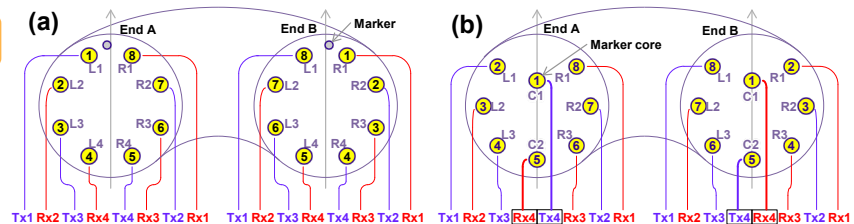


Fig. 2. MCF core layouts (a) compatible and (b) incompatible with identical FIFO routing and TRx layout at different ends. Black digits: unique core ID, black arrows: the center lines with a key direction, and $L_n/R_n/C_n$: connection core ID.

maintenance troublesome especially for high fiber count multipoint-to-multipoint networks like data center networks.

3.2. Preferable crosstalk level

One might think that lower XT always better for uncoupled MCFs to realize higher transmission capacity, but it is not the case because, to suppress the XT, we have to sacrifice A_{eff} to achieve higher light confinement in each core and/or sacrifice core density to achieve lower power overlap between the core modes. Thus, too much suppressed XT means too small A_{eff} and/or too coarse core layout [8–13], which results in a lower fiber capacity. So, there are optimum XT levels depending on transmission systems both in unidirectional and bidirectional transmissions.

3.2.1. Repeated coherent transmissions

In repeated systems, the XT-induced OSNR degradation in dB is dependent on the fiber parameters (loss, dispersion, A_{eff} , etc.) and system parameters (span length, amplifier NF, total signal bandwidth, etc.)—which affect ASE and NLI—, but independent of the span count or transmission distance [8,12,14]. So, one can optimize MCF designs in view of XT-induced OSNR penalty regardless to the total link length of the systems [8,14]. At the optimum launch power of nonlinear Shannon limit, OSNR penalty can be suppressed to 0.1 dB with the XT level of around -70 to -60 dB/km [8] (“dB/km” denotes XT at 1-km propagation and XT grows linearly, or 10 dB/decade). The penalty in capacity or aggregate spectral efficiency (SE) weakly depends on the link length, but the capacity or aggregate SE of MCFs can be maximized with the XT of -60 to -50 dB/km for the link length from 80 or 100 km to 100 folds of them [10,12], where the XT suppression and A_{eff} enhancement are well balanced in terms of the capacity.

3.2.2. Short-reach IM-DD transmissions

In short-reach IM-DD transmissions, ASE and NLI noises are not dominant, but the link length independent noises—like signal distortion due to TRx imperfection and thermal noise of photodetectors—are non-negligible. So, the optimum XT level seems still under discussions, but various studies have reported that XT of -40 dB or lower is sufficiently low for PAM-4 transmissions from theoretical analysis [15] and transmission experiments [16,17].

3.2.3. Bidirectional transmission

The XT in bidirectional transmission (XT_{bidir}) is dominantly induced by (a) Rayleigh backscattered XT (XT_{bs}) and (b) back reflected XT (XT_{refl}) from the counter-propagating light in the nearest neighboring cores, and (c) indirect XT via nearest neighboring cores (XT_{indir}), which are schematically shown in Fig. 3. All of these XTs are much lower than the direct XT between nearest neighboring cores (XT_{dir}) in practical ranges. XT_{bs} and XT_{indir} should be considered in the long-haul transmissions, and XT_{refl} and XT_{indir} in short-reach transmissions.

Based on [2], we can express the backscattered XT per span ($XT_{\text{bs,span}}$) as:

$$XT_{\text{bs}}|_{L=L_{\text{span}}} \approx XT_{\text{dir}}|_{L=L_{\text{span}}} \frac{S\alpha_R}{\alpha} \left[\frac{\sinh(\alpha L_{\text{span}})}{\alpha L_{\text{span}}} - \exp(-\alpha L_{\text{span}}) \right], \quad (1)$$

by assuming $XT_{\text{dir}} \approx h_{12}L \ll 1$ where h_{12} is the power coupling coefficient from core 2 to core 1, L_{span} is the span length between repeaters, S is the proportion of the Rayleigh scattering component recaptured into a backward direction, α_R is the Rayleigh scattering loss coefficient, α is the propagation loss coefficient of optical intensity. The loss coefficients α_R and α can be converted to decibel parameters by multiplying $10/\ln 10 \sim 4.34$. Under the Gaussian field approximation, S is expressed as $S \approx 3/(2k^2n^2w^2)$ [18] where $k = 2\pi/\lambda$, n is the refractive index, w is the spot size. For non-Gaussian field, the integral expression of S was derived in [19]. Not explicitly shown in [19], but we can rewrite the integral expression in the more useful form using effective area (A_{eff}) as

$$S \approx 3\pi/(2k^2n^2A_{\text{eff}}) = 3\lambda^2/(8\pi n^2A_{\text{eff}}). \quad (2)$$

XT_{bs} nonlinearly accumulates in each span, but grows linearly with the number of spans.

XT_{refl} can be expressed as

$$XT_{\text{refl}}|_{L=L_{\text{link}}} \approx \sum_n 2h_{12}L_nR_n \exp(-\alpha L_n) \approx 2h_{12}L_{\text{link}}R_{\text{TRx}} \exp(-\alpha L_{\text{link}}) = XT_{\text{dir}}|_{L=L_{\text{link}}} 2R_{\text{TRx}} \exp(-\alpha L_{\text{link}}), \quad (3)$$

with L_n and R_n denoting the longitudinal position and reflectivity of n -th reflection point. Because the reflection of connectors is sufficiently low ($\ll -40$ dB) [20], the reflection at transceiver (R_{TRx}) is the dominant reflection source in short reach links (e.g., the maximum reflectance at TRx is specified as -26 dB in 400GBASE-FR4/LR4 [21]). Thus, XT_{refl} can be at least 23-dB lower than ($\ll 2R_{\text{TRx}}$ -times) XT_{dir} .

By assuming $h_{12}L \ll 1$ and $h_{23}L \ll 1$, XT_{indir} from core 3 to core 1 via core2 can be approximated as [4]:

$$XT_{\text{indir,123}}|_{L=L_{\text{link}}} \approx h_{12}h_{23}L_{\text{link}}^2/2 = XT_{\text{dir,12}}XT_{\text{dir,23}}/2|_{L=L_{\text{link}}}. \quad (4)$$

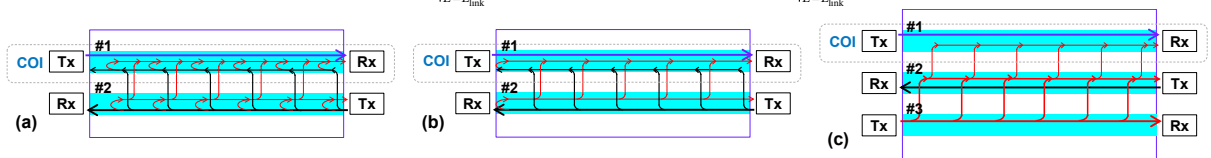


Fig. 3. Schematics of XT in bidirectional transmission: (a) Rayleigh scattered XT and (b) reflected XT from the nearest neighboring core, and (c) indirect XT via the nearest neighboring core. (COI: Channel of interest, #1–#3: core ID)

So, if $XT_{dir,12} = XT_{dir,23} = -20$ dB, $XT_{indir,123}$ is -43 dB. XT_{indir} grows quadratically with link length. By considering inter-core skew and limited memory length of Rx DSP, we should also take care of XT_{indir} originated from the channel of interest (e.g., $XT_{indir,121}$ in the case of Fig. 3(c)). If counter-propagating light can be eliminated by isolator in each repeater, XT_{indir} increases quadratically within each span but grows linearly with the number of spans.

Fig. 4(a) shows example XT_{bidir} in long-haul transmission over a 2-core fiber. The fiber parameters are also shown in the graph. The loss variation in practical range has no significant impact on XT_{bs} plots. XT per span [dB] in both axes can be translated into XT [dB/km] by subtracting $10\log_{10}(L_{span}[\text{km}]) \sim 17\text{--}20$ dB for $L_{span} = 50\text{--}100$ km. So, XT_{bidir} of -70 to -50 dB/km can be achieved by XT_{dir} of -48 to -32 dB/km. Fig. 4(b) shows XT in short-reach bidirectional transmission over square-layout 4-core fiber with -26 dB reflectance at TRx. The total XT_{bidir} of ≤ -40 dB/link can be achieved with core-to-core XT_{dir} of about ≤ -23 dB/link. Thus, we can significantly relax the XT requirements for larger fiber capacity in both long-haul and short-reach transmissions.

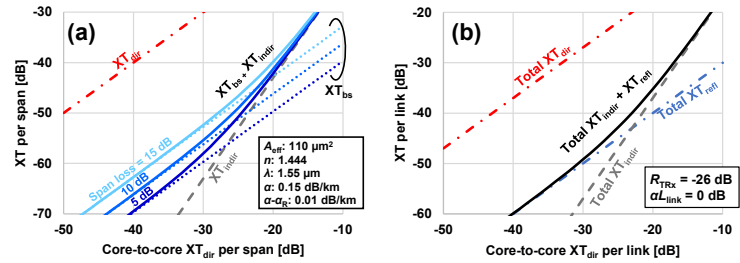


Fig. 4. XT in (a) long-haul bidirectional transmissions in 2-core fiber, and (b) short-reach bidirectional transmissions in square-layout 4-core fiber.

4. MCFs applicable to bidirectional transmissions

Table 1 summarizes the characteristics of MCFs suitable for bidirectional transmissions. The long-haul 2CF and 4CF already have sufficiently low XT_{dir} but bidirectional transmissions can make XT_{bidir} almost negligible. So, the room for XT relaxation can be used to achieve larger A_{eff} for better linearity, or tighter core pitch for better rotation misalignment tolerance. For the short-reach MCFs, the square- and trapezoidal-layout 4CFs were fabricated using simple G.652/G.657.A1 compatible cores. The square 4CF has $XT_{bidir} \leq -40$ dB/10km at 1550 nm, which provides future compatibility to wavelength band migration from O-band to C-band. The other short-reach MCFs are optimized for O-band transmissions and have $XT_{bidir} \ll -40$ dB/10km at 1310 nm. The trapezoidal 4CF realizes core identification without additional marker and easier rotational alignment. The 1x4CF can pack 8.6- μm MFD cores on a linear array in the 125- μm cladding and can be coupled to PLC-based FIFO (i.e., simple waveguide pitch converter) and edge couplers of photonic integrated circuits. Heterogeneous index trench thickness also realizes core identification without additional marker. The circular-layout 8CF can support PSM4/DR4 full duplex transmissions in one strand of 125- μm -cladding fiber.

As discussed, bidirectional transmission over an MCF is a very promising way to realize performance-improved practical MCF transmission systems with a limited MCF cross section.

Table 1: Uncoupled MCFs with a 125- μm cladding suitable for bidirectional transmissions [4,7,22,23].

Applications	Long-haul		Short-reach				
Fiber ID	2CF	4CF	Square-layout 4CF	Trapezoidal-layout 4CF	1x4CF	Circular-layout 8CF	
Cross section							
Core identification	By marker	By marker	By marker	By core layout	By trench thickness	By marker	
Core pitch λ	50 μm	44 μm	40 μm	37 μm	25 μm	~ 30 μm	
Cable cutoff λ	1461 nm ^b	1485–1510 nm	1239–1244 nm	1129–1159 nm	1060–1186 nm	1199–1219 nm	
Operation λ (λ_{op})	1550 nm	1550 nm	1310 nm	1550 nm	1310 nm	1310 nm	
A_{eff} / MFD at λ_{op}	A_{eff} 112–113 μm^2	A_{eff} 88–89 μm^2	MFD 9.0 μm	-	MFD 8.6–8.9 μm	MFD 8.4–8.7 μm	MFD 8.4–8.7 μm
Loss at λ_{op}	0.162–0.163 dB/km	0.169–0.172 dB/km	0.327–0.329 dB/km	0.194–0.197 dB/km	0.321–0.325 dB/km	0.317–0.359 dB/km	0.360–0.395 dB/km
XT_{dir} at λ_{op}	-82 dB/km ^b	-66 dB/km	-58 dB/10km	-26 dB/10km	-42 to -41 dB/10km	-40 to -35 dB/10km	-43 to -40 dB/10km
Total XT_{bidir} at λ_{op} ^a	-81 dB at 100km span ^b	-63 dB at 100km span	-84 dB at 10km	-47 dB at 10km	-68 to -65 dB at 10km	-66 to -59 dB at 10km	-69 to -66 dB at 10km
Related Ref.	[7]	[22]	-	-	-	[4,23](new fabrication)	

a) calculated from XT_{dir} using (1–4), b) design calculation

This research was supported in part by the National Institute of Information and Communications Technology (NICT), Japan.

References

- [1] T. Ito et al., in *OFC 2013*, OTh3K.2.
- [2] A. Sano et al., *JLT* **32**(16), 2771 (2014).
- [3] Y. Geng et al., in *Proc. SPIE*, p. 939009.
- [4] T. Hayashi et al., *JLT* **34**(1), 85 (2016).
- [5] M. Arikawa et al., *JLT* **34**(8), 1908 (2016).
- [6] T. Gonda et al., in *OECC/PS 2016*, MC1-3.
- [7] Y. Tamura et al., in *OFC 2019*, M1E.5.
- [8] T. Hayashi et al., *Opt. Exp.* **20**(26), B94 (2012).
- [9] T. Hayashi and T. Sasaki, in *IEEE Photonics Society Summer Topicals 2013*, MC2.4.
- [10] T. Nakanishi et al., in *OFC 2015*, Th3C.3.
- [11] R. S. Luis et al., in *Advanced Photonics 2017*, NeTu2B.2.
- [12] J. M. Gené et al., *PTL* **31**(9), 673 (2019).
- [13] J. M. Gené et al., in *ECOC 2019*, M.1.D.5.
- [14] R. S. Luis et al., *J. Sel. Top. Quantum Electron.* **26**(4), Art no. 4400609 (2020).
- [15] C. H. Kim, *OL* **44**(24), 5965 (2019).
- [16] K. Benyahya et al., in *ECOC 2019*, W.3.A.3.
- [17] K. Li et al., in *OECC 2021*, M3F.3.
- [18] E. Brinkmeyer, *Electron. Lett.* **16**(9), 329 (1980).
- [19] A. Hartog and M. Gold, *JLT* **2**(2), 76 (1984).
- [20] T. Morishima et al., in *OFC 2020*, Th31.2.
- [21] IEEE Std 802.3cu-2021.
- [22] H. Sakuma et al., in *EXAT 2019*, P-3.
- [23] T. Hayashi et al., in *IWCS 2018*, P-6.